Proceedings of the 37th IAHR World Congress
August 13 – 18, 2017, Kuala Lumpur, Malaysia

LABORATORY EXPERIMENTS OF PULSED SUBAQEOUS SEDIMENT DENSITY FLOWS: INTERNAL STRATIFICATION AND LAYERING

MARIANGELA SFOUNI-GRIGORIADOU[(1)], CARMELO JUEZ[(2)], MARIO J. FRANCA[(3)] & BENOIT SPINEWINE[(4)]

[(1,4)] Fugro GeoConsulting, Brussels, Belgium,
m.sfouni@fugro.com
[(1,4)] Department of Civil Engineering, Université catholique de Louvain, Louvain-la-Neuve, Belgium,
[(2,3)] Laboratory of Hydraulic Constructions, École Polytechnique Fédérale de Lausanne, Lausanne, Switzerland

ABSTRACT

This paper reports on an experimental study which focuses on reproducing small scale sediment density flows in a laboratory flume. The observations are aimed at improving the parametrization of the relations that govern the transition between different phases of the flows. Dense mixtures of plastic sediment of variable grain size (thermoplastic polyurethane) and water were fed into the water-filled flume by gravity from a supply tank. Different grain-size and slope combinations were examined and the resulting velocity fields were obtained using UVP (Ultrasonic Velocity Profile) at various points along the channel. The flow was imaged through the transparent sidewall to track the velocity of the flow head for each test case. Image analysis also allowed a qualitative characterization of the vertical density stratification and water entrainment during runout. The runout distance and flow thickness are used to highlight the differences in the dynamic behavior of the flow for each test case. Data gathered from the experiments will be exploited in the further development of predictive numerical models for slide-induced debris flows transitioning to turbidity currents.

Keywords: Debris flow; density flow; mass movement; submarine landslide; turbidity current.

1 INTRODUCTION

Submarine debris flows and turbidity currents constitute a major geohazard as they are capable of transporting vast quantities of soil at significant velocities down channels and escarpments in deep-water environments. As subsea infrastructure continuously develops, a proper assessment of the risk of impact from these types of flows becomes increasingly important. The understanding of the internal processes governing the dynamics of these mass transport events, which are intrinsically transient and stratified, is critical.

The transition from a dense debris flow to a dilute turbidity current, as a result of downslope propagation and interaction with the sea floor and ambient sea water, can be divided into three main phases: (i) the initial failure and break-up of blocks and slumps, (ii) the transformation of the released material to a viscoplastic fluid and the development of a debris flow, and (iii) the generation of a turbidity current due to friction and mixing at the top interface of the debris flow producing a cloud of dilute suspended matter (Locat and Lee, 2005).

A predictive model of turbidity current generation from submarine debris flows was presented by Mohrig and Marr (2003). Their laboratory experiments confirmed that the influence of the dynamic stresses, developed at the very fronts of the parent debris flows, on the turbidity current development depends on their magnitude relative to an effective yield strength for the parent mixture of sediment and water (Mohrig and Marr, 2003).

Felix and Peakall (2006) worked on lock exchange experiments to study the generation of turbidity currents from debris flows. The transformation of debris flows occurs through multiple processes like erosion of the dense mass, breaking apart of the dense underflow, breaking of internal waves and turbulent mixing. Some of these processes take place simultaneously in a flow event, while others occur at different phases and positions. It was observed that a more efficient transformation to a turbidity current layer occurs for less-cohesive debris flows (Felix and Peakal, 2006).

Zakeri et al. (2010) studied the process in which a submarine debris flow and the overriding turbidity form the seabed deposits and how the deposits relate to the parent flow. In a series of flume experiments, slurries with different clay content were tested.

The experiments presented in the current work are focused on triggering dense subaqueous debris flows in a laboratory flume, and monitoring their propagation and associated degree of mixing and dilution. The effects of sediment size and bed slope on the propagation and the internal stratification of such flows are investigated. Two superposed layers are seen to coexist, a dense basal layer and a dilute top layer, which we interpret as a debris flow and a turbidity current, respectively. It is expected that the obtained dataset will provide a validation database for the development of a two layer depth-integrated mode of subaqueous landslides, currently in development.

The details of the experimental set-up are presented in section 2. Section 3 focuses on the instrumentation and processing of acquired images. Section 4 details the experimental procedure, and results are presented in section 5.

2 EXPERIMENTAL SET-UP

The experiments were conducted in a flume of 2.7 m long, 0.14 m wide and 0.21 m deep, with a variable bottom slope at the Hydraulic Constructions Laboratory of the École Polytechnique Fédérale de Lausanne (Figure 1). The glass-plastic flume can be tilted using adjustable supports at slopes ranging from 0% to 4.4%. The flume was initially filled with fresh water. Due to the water free surface, the maximum attainable water depth decreases in the upstream direction when the flume is tilted.

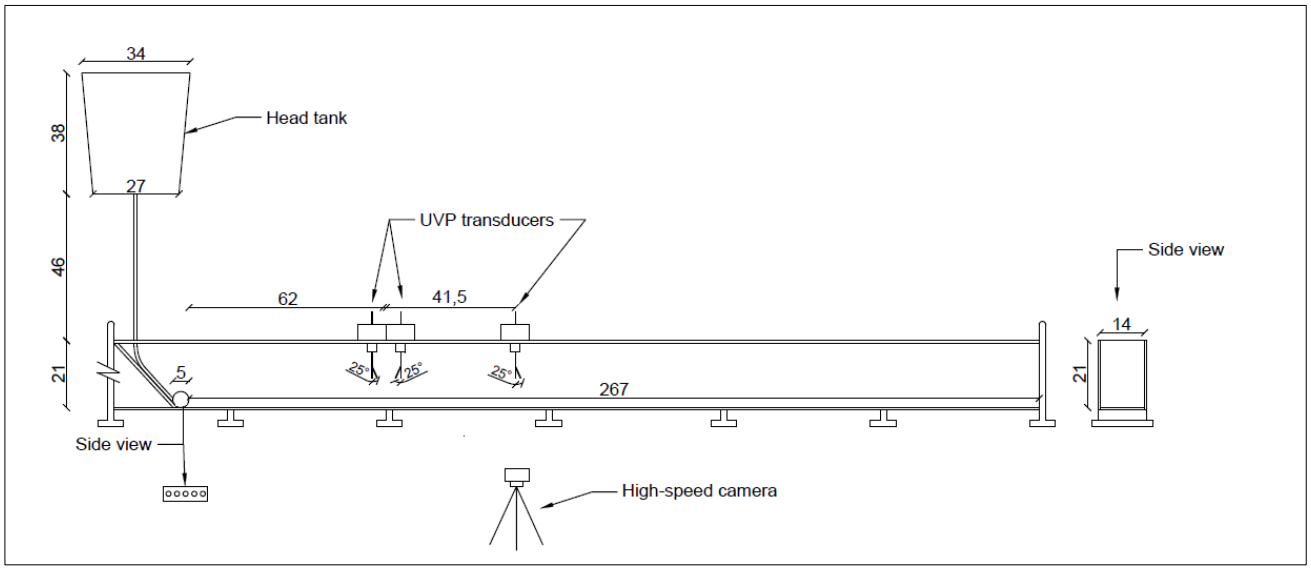

Figure 1. Sketch of the experimental set-up. All dimensions are in centimeters.

Mixtures of plastic sediments (thermoplastic polyurethane) and water were fed into the flume from an eight-litre head tank through a plastic tube ending in a perforated screen, to ensure uniform release of the material across the flume width. The sediment mass concentration in the head tank was set equal to 30% for most experiments. This percentage indicates a high density flow that could potentially reproduce the behavior of a debris flow. A few experiments were performed with a reduced initial sediment mass concentration equal to 8%.

Three different grades of sediment were used, with a median diameter (D_{50}) of 80 µm, 160 µm and 200 µm, respectively. For each sediment grain size, three different channel slopes were investigated. For each slope, an additional experiment was performed with a mixture of equal parts of sediments with D_{50} of 80 µm and 200 µm (Table 1).

In overall, the combinations of channel slope, sediment mixture, and initial sediment concentration resulted in a total of 15 individual experiments, as detailed in Table 2.

Table 1. Characteristics of the sediments.

Sediment name	D_{50} (µm)	Density (g/cm^3)
S	80	1.16
M	160	1.16
L	200	1.16

Table 2. List of experiments.

Experiment name	Sediment Type	Slope (%)	Mass Concentration (%)
S1	S	0	30
M1	M	0	30
L1	L	0	30
MIX1	50%S + 50%L	0	30
TC1	M	0	8
S2	S	2.2	30
M2	M	2.2	30
L2	L	2.2	30
MIX2	50%S + 50%L	2.2	30
TC2	M	2.2	8
S3	S	4.4	30
M3	M	4.4	30
L3	L	4.4	30
MIX3	50%S + 50%L	4.4	30
TC3	M	4.4	8

3 INSTRUMENTATION

3.1 Velocity measurement

Velocity profiles were measured using an Ultrasonic Doppler Velocity Profiler (Met-Flow, UVP). Three transducers have been immersed near to the water surface at an angle of 25° to the normal of the flume bottom. The position of the transducers is illustrated in Figure 1. The basic frequency of the transducers for the emitting ultrasonic pulse was 4 MHz. The velocity resolution of UVP DUO was set at 0.764 mm/s and its spatial resolution was set at 0.74 mm. A fixed number of 128 points were measured in each profile and the sampling period was equal to 0.161 s. The measurements gave the projected vertical profiles in the middle of the width of the flume. Each of the three UVPs was interrogated in sequence with a multiplexer throughout the duration of the experiment, and the time interval between successive measurements at a given transducer is in the order of 2.3 s.

3.2 Flow imaging and image processing

The flow was observed through the transparent side wall of the flume. A SMX-160 camera with acquisition frequency of 10 frames per second was used to obtain gray scale digital images with a resolution of 2208 by 400 pixels. The position of the camera is illustrated in Figure 1. On average 350 frames were taken for each experiment.

Four steps of image processing are applied to the raw images. First, the images are ortho-rectified using a number of reference points with known coordinates to correct for image distortion, and the resulting ortho-rectified image is resampled at a resolution of one pixel per mm, with the x-axis being defined as streamwise, tilted along-slope direction, and the y-axis orthogonal upwards. Second, a correction is applied to account for uneven illumination of the flow from the single light source used. A bell-shaped brightness correction factor is applied, which is calibrated on the basis of the observed illumination of a reference plate along the bottom of the flume sidewall. Third, the image background is removed by subtracting the initial image, prior to flow initiation, from the entire image sequence. Due to the bright color of the plastic sediment used, the current appears on the resulting image sequence as variable shades of grey on a perfectly black background, and the local brightness of the flow is, to a good approximation, a direct proxy for the local sediment concentration at that location. Lastly, for better visualization, the grey image is transformed into a color image with a jet color map featuring variations of blue-green-yellow-red shades that highlight regions of dense and dilute flow. The color map is altered so that the image regions indiscernible of the image background (with a pixel value of zero) are painted white for better visualization of the limits of the propagating current.

4 EXPERIMENTAL PROCEDURE

All the mixtures were prepared using a mixer device in order to ensure the uniformity of the mixture. The flume was filled with fresh water. The flume water and tank mixtures had approximately the same temperature, therefore temperature effects are considered negligible in the flow dynamics. When the mixing procedure was completed, the resulting mixture was immediately released in the head tank to avoid any settling of the sediments, and discharged into the flume under gravity. The gradual lowering of the mixture level in the head tank was tracked with another camera, and was roughly constant for all experiments with a total emptying duration of ~25 s, which corresponds to a feeding discharge of ~1/3 L/s. The release of the mixture was synchronized with the start of the UVP measurements. Simultaneously, the recording with the digital camera was triggered. After each experiment, the flume was drained out and refilled with fresh water prior to the next experiment.

5 RESULTS

5.1 General down-channel evolution

Preliminary results are presented in this paper for the configuration with a bed slope of 4.4%, and an initial mass concentration of sediment equal to 30% and composed solely of the larger sediment size of 200 μm. Analysis for the other configurations is ongoing and will be reported at a later stage.

Figure 2 shows snapshots of the current evolution at selected instants after release. As discussed in section 3.2, pixel values on the processed images are a good proxy for local sediment concentration in the current; however, in the absence of a robust calibration, the correlation cannot be precisely constrained and therefore the pixel brightness is presented in digital values rather than sediment concentration in percent. Nevertheless, what appears in shades of red color on the processed images is considered as a dense flow, while shades of yellow, green, cyan and blue correspond to gradually more dilute sediment suspensions.

The sequence of images on Figure 2 reveals the general down-channel propagation of the current, the preservation of a relatively dense and thick current head followed by a region where the dense basal layer is thinner, and the distinctive pattern of billows that govern the dilution of the top layer of the current and the formation of a turbidity cloud.

The current head is seen to preserve a density in the order of that in the most upstream section of the current. Mixing with the ambient fluid is initiated at the top of the head region, but the resulting turbidity is simultaneously slowed down and therefore trails behind the front, while additional dense current is fed into the frontal head from the basal layer, allowing it to remain dense. The sediment concentration in the front and dense basal layer is however not expected to be as high as 30% as in the head tank, but more probably in the range of 10 to 15%. This is due to immediate turbulent mixing at the exit of the perforated tube ending. A more robust calibration of the brightness-to-concentration correlation is planned for future experiments to confirm this.

Behind the front, the generation of lower density turbidity is quite apparent on the images, and is a result of large-scale mixing processes with the ambient water.

5.2 Frontal velocity

Visualization of the current head on the ortho-rectified images allows tracking the front position and velocity in time. These are presented in Figure 3, with readings of the front position on the left vertical axis and front velocity on the right vertical axis. The current is propagating with linearly increasing velocity for a duration of 30 s while for the last 5 s it has a constant velocity until the flow reaches the end of the flume. The maximum velocity is approximately 72 mm/s.

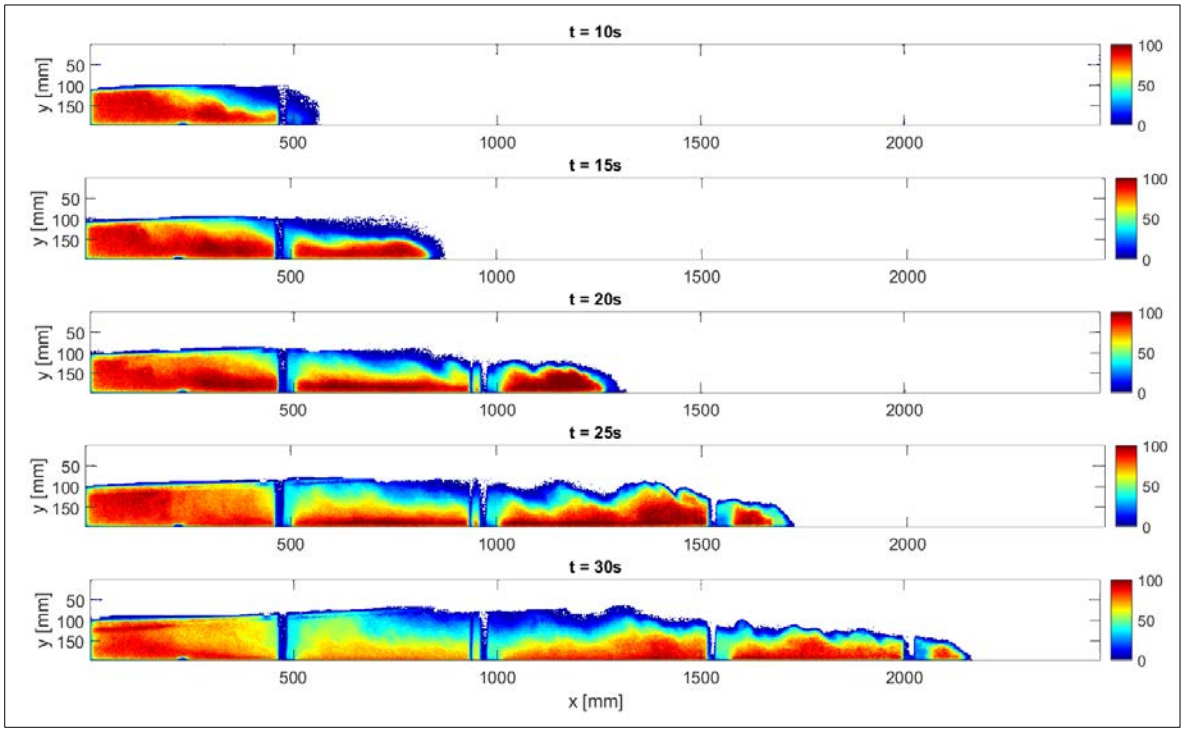

Figure 2. Snapshots of the flow for the test with a slope of 4.4% and 200μm grain size. Dashed lines define regions where the existence of shadows do not allow proper illumination of the flow.

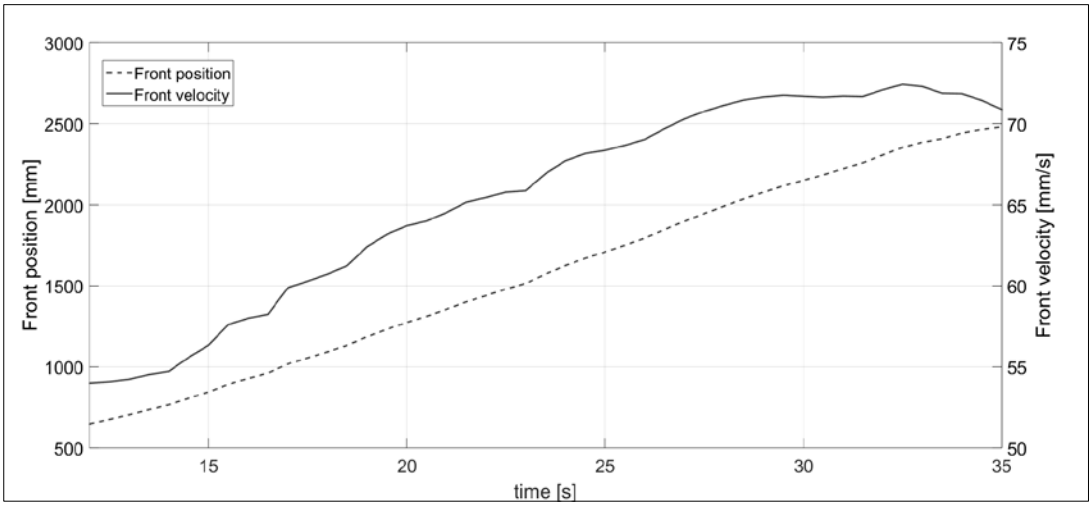

Figure 3. Time evolution of the front velocity (solid line, right axis) and position (dashed line, left axis).

5.3 Velocity and density stratification

The aim of this work was to investigate the internal stratification and layering of dense subaqueous sediment flows, by simultaneously measuring velocity and density profiles. This appears possible for the present experiments by combining the UVP velocity profiles and the qualitative density information encapsulated in the brightness of the digital images, interrogated at the same position than the UVP probes.

In Figure 4 to Figure 7, the downstream velocity and the brightness profiles are presented for selected time instants at the location of the third transducer (x = 910mm).

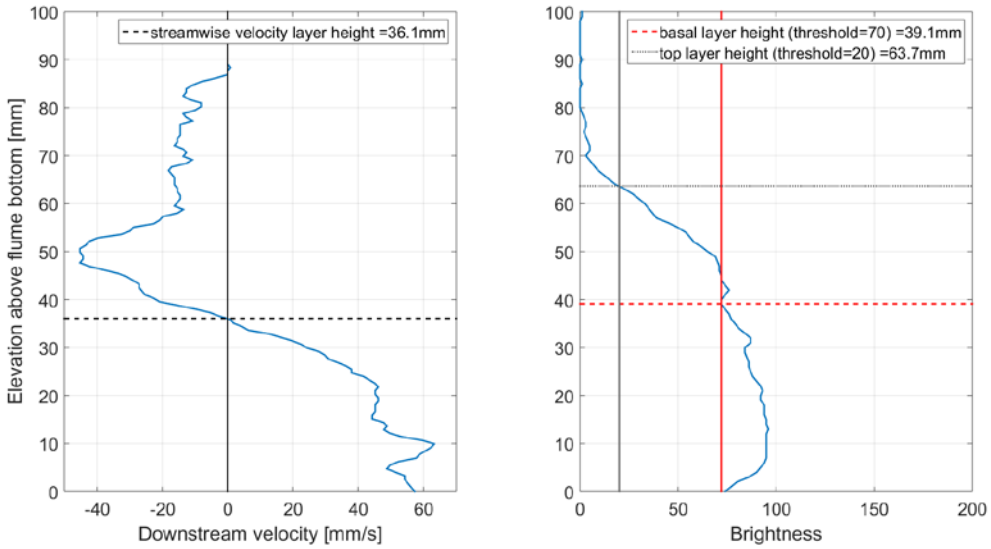

Figure 4. Downstream velocity and brightness profiles at position x = 910 mm and time t = 18.3 s.

On all velocity profiles (left panels), the height corresponding to a zero streamwise velocity is highlighted by a dashed line. While the bottom layer propagates down the channel, the top portion of the current propagates in the opposite direction. This is a direct result of the fact that the current is propagating in an enclosed basin, and any current in one direction must be balanced by an opposite current in the other direction, with only minor deviations possible that result from the generation of mild free surface waves at the flume free surface. Due to the limited depth available in the flume, the backward current incorporates some of the turbidity generated at the top of the density current.

The density/brightness profiles shown on the right panels of the figures reveal a pattern of upward stratification, with the brightness decreasing to zero at the top of the current. A qualitative partition of the current in a dense basal current and a dilute top current can be made by adopting a brightness threshold of 70, which corresponds to orange color on the flow images of Figure 2 and is slightly smaller than the maximum observed brightness. On Figure 4 to Figure 7, it is observed that this partition based on density corresponds quite well with the partition between down-channel and reverse currents based on the velocity profiles.

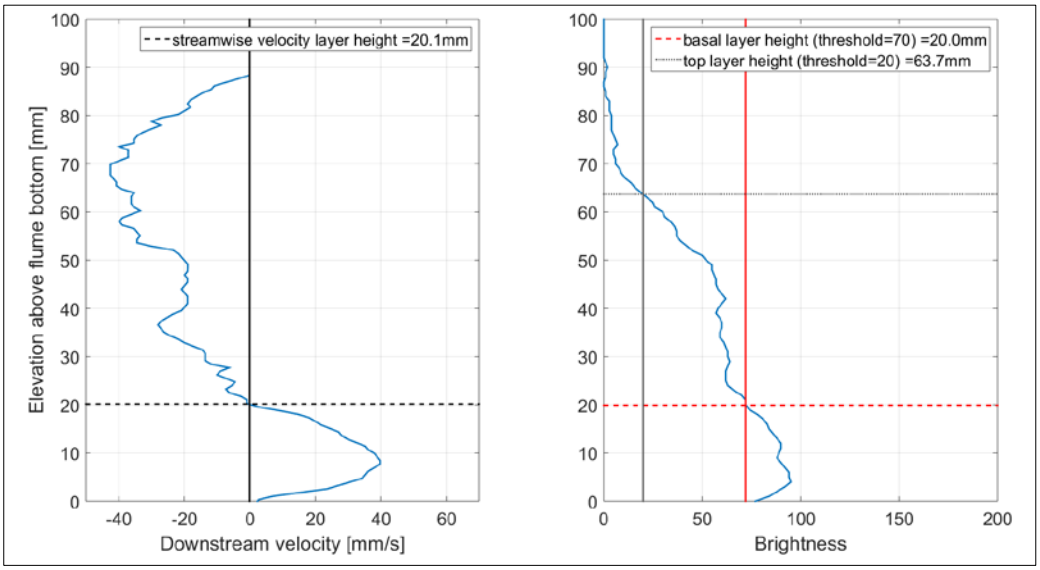

Figure 5. Downstream velocity and brightness profiles at position x = 910 mm and time t = 20.6 s.

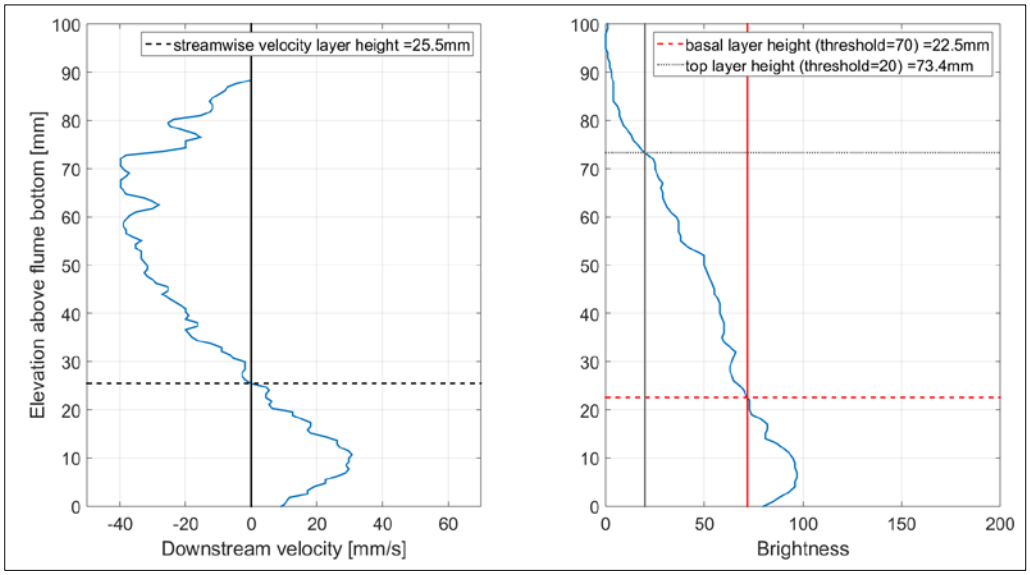

Figure 6. Downstream velocity and brightness profiles at position x = 910 mm and time t = 22.9 s.

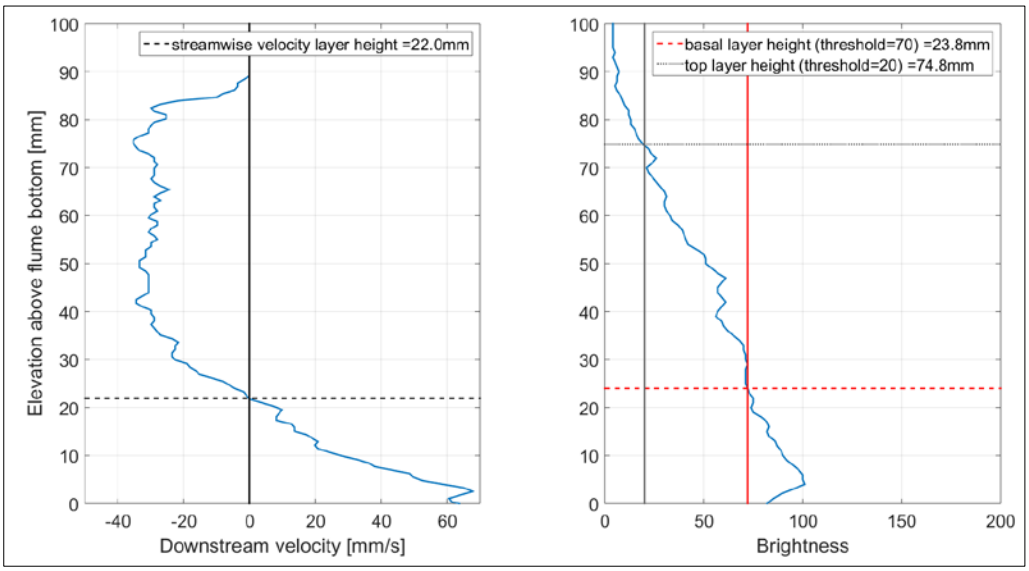

Figure 7. Downstream velocity and brightness profiles at position x = 910 mm and time t = 25.2 s.

This suggests indeed that the flow can be abstracted into two distinct layers: a basal layer that remains dense and rapid and dictates the down-channel propagation of the density current, and a top layer, which is much more dilute as a result of mixing, and propagates at a much slower velocity – which in the present case may result in backward velocity due to the lock-exchange configuration and the finite water depth in the flume.

Flow brightness profiles for different time instances at the same location x = 910 mm are given in Figure 8. At t = 15 s, the flow has not reached this location yet as it is evidenced by the near zero values of brightness. The very front of the flow passes from the location of the transducer at t = 16 s and is characterized by the low brightness values. Immediately after, the denser part of the flow head passes, with a thickness of circa 40 mm having a brightness above the adopted threshold of 70. From time t = 18.3 s to 25.2 s, the thickness of the dense layer of the flow is decreasing, while the total flow thickness is increasing due to the growth of the turbidity cloud. Passed t = 30 s, the dense layer has vanished but the total flow thickness surpasses 120 mm.

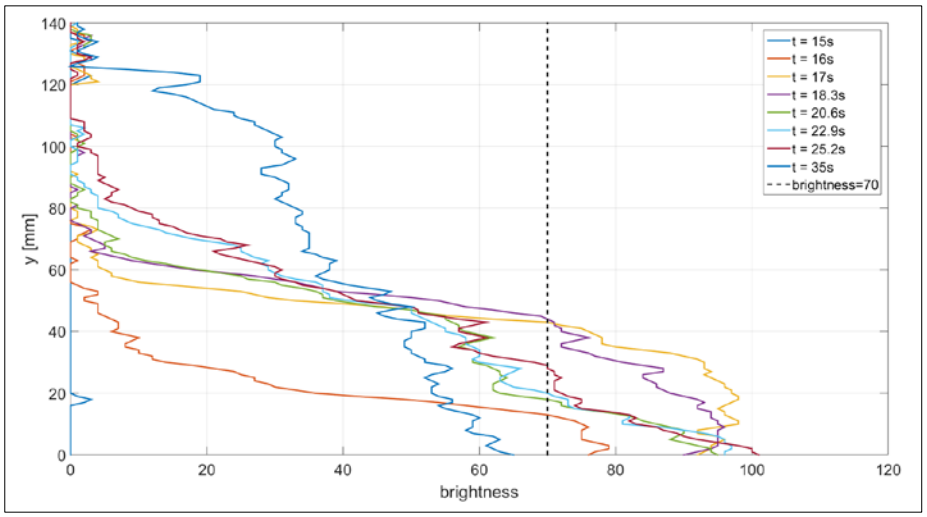

Figure 8. Brightness profiles for different time instances at position x = 910 mm.

A second threshold can be considered to investigate stratification, which distinguishes the dilute turbidity cloud from the background water. A brightness threshold of 20 is adopted for that purpose. The associated levels are also shown on the right panels of Figure 4 to Figure 7. By applying the same methodology to all images, on the top panel of Figure 9 the time evolution of the thickness of the dense and basal layers, with respective thresholds of 20 and 70, is presented, along with intermediate contours at multiples of 10. The lower panel of Figure 9 shows the fraction of the flow thickness that is occupied by the dense basal flow. The dense flow initially occupies roughly 90% of the flow thickness, while toward the end of the experiment it vanishes to zero as the dilute turbidity current thickens and the dense flow stops.

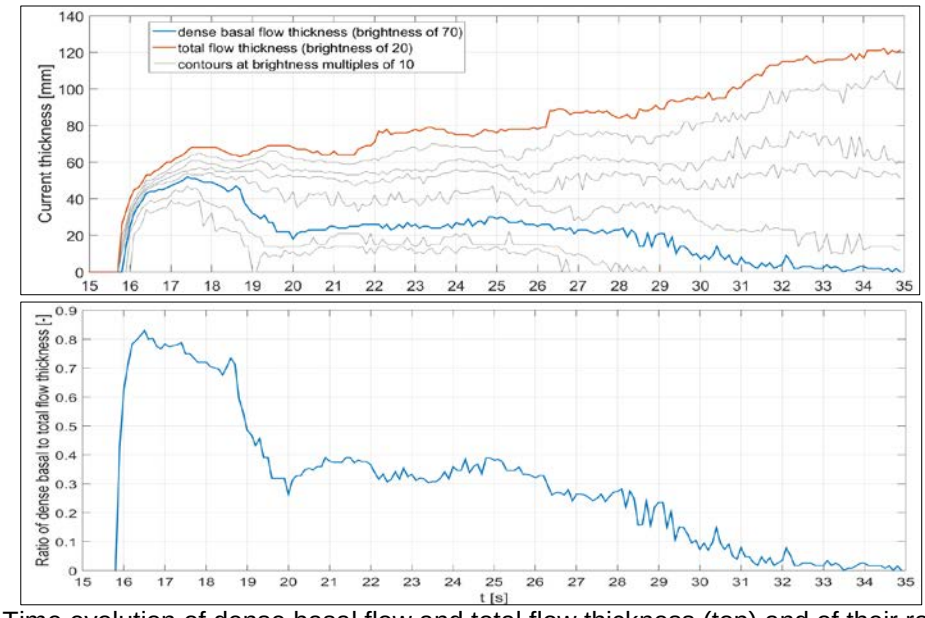

Figure 9. Time evolution of dense basal flow and total flow thickness (top) and of their ratio (bottom).

5.4 Space-time visualization of depth-integrated quantities

The density flows investigated in the present experiments may be considered as shallow flows, in the sense that their development in the streamwise direction is more than an order of magnitude larger than their thickness. It is therefore of interest to derive depth-integrated quantities. Figure 10 and Figure 11 show the space-time evolution of the flow thickness and depth-averaged flow brightness, respectively. The flow thickness is here defined as the portion of the current whose brightness is larger than the previously set threshold of 20 distinguishing the turbidity cloud from the surrounding clear water. In Figure 10, the highest density is observed near to the front of the flow. As the propagation continues, mixing starts to develop immediately behind the front and the thick mixing billows recirculate backwards, as can be seen from the curved trajectories of the regions of thick flow in Figure 10. The brightness is then averaged over the current thickness to yield the values reported in Figure 11. In that figure, the dense region of the current head and the "ejection" events associated with the formation of mixing billows are also clearly identified.

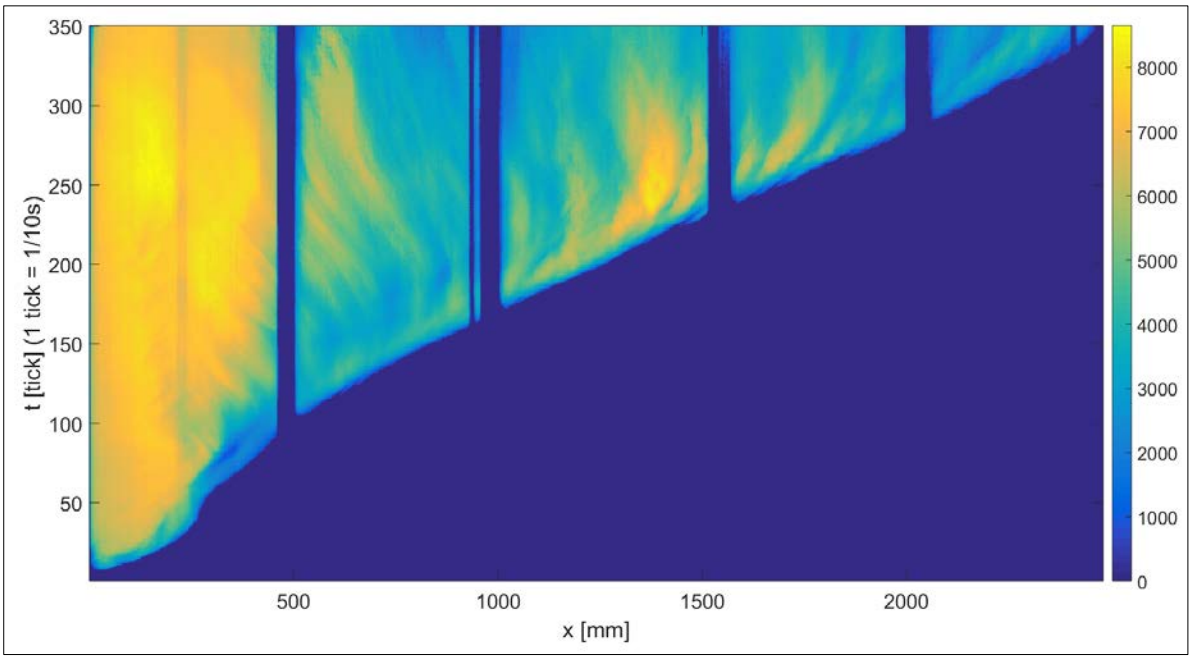

Figure 10. Flow thickness (defined as all pixels brighter than a set threshold of 20).

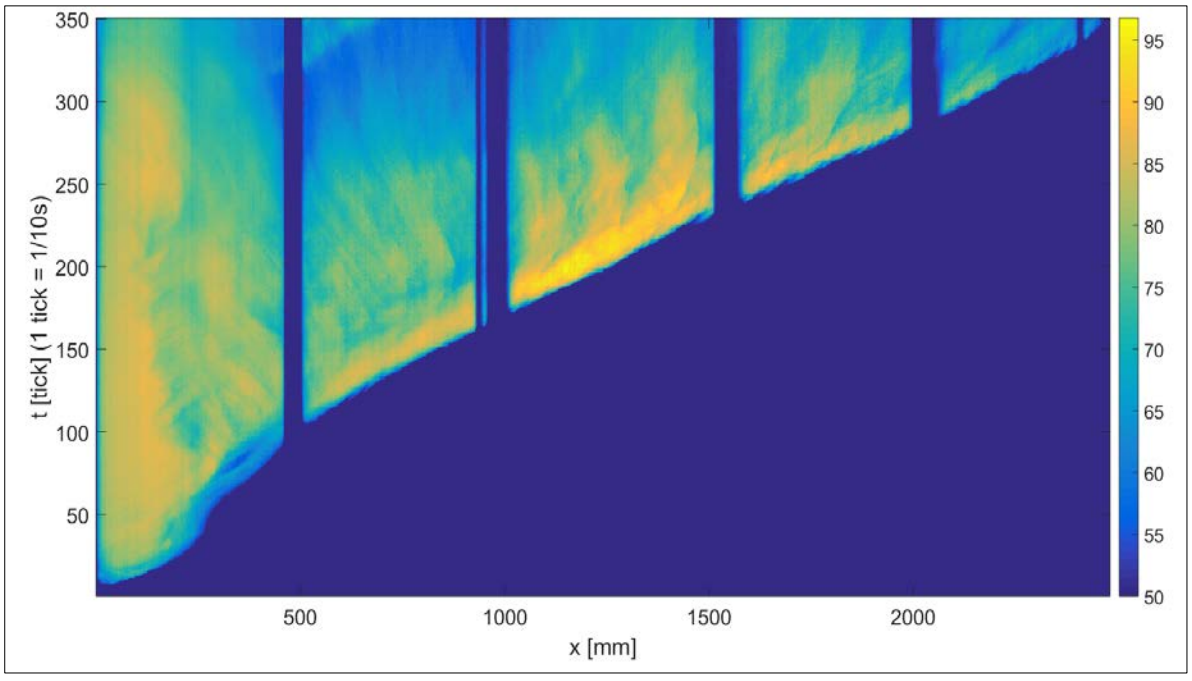

Figure 11. Depth-averaged flow brightness (averaged over flow thickness).

6 CONCLUSIONS

In this study, the behavior of subaqueous sediment density flows was investigated. Plastic sediment-water mixtures of different grain sizes were tested in a series of flume experiments with varying bed slopes. Velocity profiles were acquired at selected positions using UVP probes. A camera captured the flow with a frequency of 10 frames per second through the transparent sidewall. The images were processed to correct for image distortion and uneven illumination, to allow tracking of the current front velocity, thickness, and brightness which is a qualitative for sediment concentration. Preliminary results, restrained to the case with a bed slope of 4.4%, sediment's median grain size of 200 μm and initial sediment mass concentration of 30 %, are presented in this paper.

Analyses of the image sequence allows to highlight the partition of the flow into a basal layer, which remains dense throughout the current propagation, and a dilute turbidity cloud resulting from mixing with ambient water at the rear of the current head. The two layers were defined using the image brightness as an indication of concentration. The brightness thresholds used for the definition of each layer, were obtained after a correlation of the brightness profiles with the velocity profiles acquired with the UVPs. The height of the bottom layer as defined by the brightness threshold coincided well with the height of the flow region characterized by streamwise velocity, indicating rapid propagation of the dense basal layer and much slower, or even reverse, velocity for the dilute turbidity cloud.

The space-time evolution of depth-integrated quantities reveals that the front of the flow remains dense throughout the experiment, suggesting that near to the front, the sediment lost to turbidity trailing behind at the top of the current is balanced by additional dense current fed from the basal layer. The formation of mixing billows results in "ejection" events with a distinctive curved path on the space-time plots.

To our knowledge, these experiments are quite unique in the sense that they allow simultaneous measurements of velocity and density within the density currents, and allow investigating their internal stratification. Performing a quantitative analysis on the entire set of test cases is ongoing, and will hopefully lead to a characterization of the dynamic behavior that governs the transition between different phases of subaqueous sediment density flows. Parametrization of the vertical stratification and water entrainment relations will be important for predictive numerical models for slide-induced debris flows transitioning to turbidity currents.

ACKNOWLEDGEMENTS

This work was funded by the ITN-Programme (Marie Curie Actions) of the European Union's 36 Seventh Framework Programme FP7-PEOPLE-2013-ITN under REA grant agreement n° 607394-37 SEDITRANS.

REFERENCES

Felix, M. & Peakall, J. (2006). Transformation of Debris Flows into Turbidity Currents: Mechanisms Inferred From Laboratory Experiments*. Sedimentology*, 53,107-123.

Locat J. & Lee H.J. (2005). *Subaqueous Debris Flows Chapter 9. Debris-flows Hazards and Related Phenomena,* Springer*,* 203-245.

Mohrig D. & Marr J.G. (2003). Constraining the Efficiency of Turbidity Current Generation from Submarine Debris Flows and Slides Using Laboratory Experiments*. Marine and Petroleum Geology,* 20(6), 883-899.

Zakeri A., Si G., Marr J.G. & Høeg, K. (2010). Experimental Investigation of Subaqueous Clay-Rich Debris Flows, Turbidity Generation and Sediment Deposition*. Submarine Mass Movements and Their Consequences* of the series *Advances in Natural and Technological Hazards Research*. D.C. Mosher (Eds.), Springer Science, 28, 105-115.

